# The separation of quantum and classical behavior in proton transfer reactions: Implications from studies of secondary kinetic isotope effects

Radu Iftimie and Jeremy Schofield*
*Chemical Physics Theory Group, Department of Chemistry,*
*University of Toronto, Toronto, Ontario, Canada M5S 3H6*
(January 4, 2002)

In this paper the separability of the nuclear degrees of freedom of system into mixed quantum and classical components is examined by looking at secondary kinetic isotope effects in a model proton transfer reaction. To explore this issue, the nature of secondary kinetic isotope effects is investigated by means of molecular mechanics and *ab initio* simulations of a model system in which intra-molecular proton transfer occurs in a region whose chemical topology is similar to that of malonaldehyde. Isotope effects are calculated using importance sampling Monte Carlo techniques designed to improve the statistical efficiency of *ab initio* simulations within the framework of quantum centroid transition state theory. The *ab initio* results for kinetic isotope effects are contrasted with those obtained using two molecular mechanics potential energy functions. It is demonstrated that the calculated isotope effects are extremely sensitive to subtle features of the potential energy surface, which suggests that information from *ab initio* structure and energy calculations about configurations along the reaction path must be utilized in the construction of classical potentials in order to obtain accurate secondary kinetic isotope effect predictions. It is also demonstrated that quantum nuclear degrees of freedom of all secondary atoms which move significantly as a chemical reaction proceeds should be treated explicitly, as even secondary heavy-atom tunneling effects could be significant.

## I. INTRODUCTION

The close connection between experimentally measurable isotope effects and the mechanism of a reaction has been frequently exploited by the physical organic chemistry community.[1] The reaction mechanism reflects the correlation between chemically reactive events and structural rearrangements or topological changes in the rest of the molecule. Experimentally, the correlations between the molecular motions can be inferred by examining the changes in reaction rate caused by isotopic substitution at different atomic centers. Studies involving kinetic measurements in experiments where both primary and secondary positions are isotopically substituted are particularly helpful in predicting reaction mechanisms.[1]

Unfortunately, experimental studies of kinetic isotope effects are limited by the small number of naturally-occurring isotopes and by the difficulty of synthesizing chemical species with a particular isotopic labeling. Computational studies of isotope effects, on the other hand, allow fictitious as well as naturally-occurring isotopic changes which permit more appreciable kinetic isotope effects to be obtained. However, the reliability of numerical calculations of isotope effects is greatly dependent on the accuracy of the method by which the electronic energy of a nuclear configuration is calculated within the Born-Oppenheimer approximation. Although accurate structures and energies of configurations corresponding to stationary points on the potential energy surface can be achieved for molecules of modest size using *ab initio* methods, the computational demand of the electronic structure calculations limits the number of configurations which can be computed in a reasonable amount of computer time. This limitation is particularly relevant to computational studies of rare events such as chemical reactions, in which the statistical resolution of rate constant calculations depends exponentially on the number of *independent* configurations obtained in the neighborhood of the transition state during the simulation.

A new method for improving the rate of exploration of state space in *ab initio* Monte Carlo (MC) simulations was recently proposed.[2] The method, termed the molecular mechanics-based importance function sampling method (MMBIF), consists of using a distribution based on a classical model potential to guide MC proposals for an *ab initio* Markov chain constructed to have the correct limiting dis-

*Electronic mail: jmschofi@chem.utoronto.ca

tribution. It was demonstrated that the utilization of a reasonably accurate molecular mechanics potential as an important function decreases the correlation of an *ab initio* MC simulation by two orders of magnitude.[2] Nuclear delocalization effects such as incoherent tunneling and zero-point vibrations can be incorporated in the MMBIF sampling of reactive state space by means of the quantum centroid transition state theory of Gillan[3] and Voth, Chandler and Miller[4] in which classical nuclei are replaced by polymer rings of harmonically-interacting beads. It was demonstrated that by combining the MMBIF method with multiple Markov chain methods for the path-integral simulation, configurations in which the reaction coordinate is essentially statistically independent are generated on average after only two MC updates.[6] The MMBIF based multiple Markov chain method is a cheaper and faster alternative to more sophisticated path-integral molecular dynamics sampling techniques[7] in *ab initio* rate constant calculations.

In this study, intra-molecular proton transfer is considered to occur in a fictitious condensed-phase system containing a "reactive core" with a chemical topology similar to that of malonaldehyde. The influence of the quantum nuclear degrees of freedom of secondary atomic centers is examined using both molecular mechanics and *ab initio* electronic structure methods in combination with imaginary-time path-integral simulation techniques. Because the influence of the solvent and of the other atoms surrounding the malonaldehyde "reactive core" is not explicitly treated in our calculations, one might expect some differences between our results and those obtained in an actual calculation of the system in a condensed-phase environment. However, it seems reasonable to assume that in a non-polar aprotic solvent the solvent atoms behave as "spectators" which have little influence on secondary kinetic isotope effects in intra-molecular proton transfer reactions.[1] Under these assumptions, the qualitative features pertaining to the influence of the quantum nuclear degrees of freedom of secondary atoms on the centroid potential of mean force of malonaldehyde should provide insight into real kinetic isotope effects in some intra-molecular proton transfer reactions for which uni-molecular rate descriptions are appropriate. Uni-molecular rate constants have been measured for multiple proton transfer reactions involving the cooperative exchange of protons between acetic acid and methanol in nonpolar aprotic solvents such as methylcyclohexane.[8]

The study of secondary isotope effects in model reactions is important in understanding the conditions under which mixed quantum-classical schemes can be applied to simplify the fully quantum-mechanical description of the nuclear motion. Since classical behavior is obtained for any atom whose mass is sufficiently large, computational studies of kinetic isotope effects provide a powerful means of analyzing the conditions in which an increase in the nuclear mass of an atom does not significantly alter the overall kinetics. Such a condition is a minimum requirement for the classical treatment of the atom. Intuitively, one might anticipate that primary atoms explicitly involved in the bond-forming and bond-breaking events should be treated within a quantum mechanical framework. However, there is less consensus on whether or not secondary atoms not *directly* involved in chemical events must be treated in a quantum mechanical fashion. One of the goals of this paper is to explore the conditions in which the quantum behavior of collective motions of secondary atoms must be considered.

In section $II$, the molecular mechanics based importance function simulation approach used when nuclear degrees of freedom are treated classically as well as quantum mechanically by means of polymer rings of beads is reviewed. In section $III$, the centroid potential of mean force results obtained using *ab initio* electronic structure methods are contrasted with results obtained using two molecular mechanics potentials. It is concluded that using molecular mechanics potentials can result in erroneous secondary kinetic isotope effects and a qualitatively incorrect picture of the reaction mechanism unless special care is exercised in their construction. Finally, it is demonstrated that in systems in which the motion of secondary atoms is significant in the transition state region, quantum mechanical tunneling of even heavy secondary atoms can be significant.

## II. *AB INITIO* MONTE CARLO IMPORTANCE SAMPLING METHODS

The calculation of approximate rate constants within the framework of transition state theory can be carried out using molecular-dynamics (MD) or Monte Carlo (MC) sampling methods. These methods consist of generating a time series of configurations by either deterministic or stochastic dynamics in which any given configuration of the system appears with a known (and desired) probability. Transition state theory rates can be constructed from the time series by forming an estimator of the reaction rate in terms of the potential of mean force along a reaction path.[2] Since the accuracy of the calculated value for the rate constant increases as the square root of the number of independent points in the activated region, it is clearly desirable to generate a

long sequence of configurations in which the correlation length of the order parameter characterizing the reaction path is as short as possible. The importance of sampling efficiency is particularly acute when only slow methods of generating the sequence of configurations are available.

Recently, Iftimie, Schofield and collaborators introduced molecular mechanics-based importance function (MMBIF) sampling schemes to improve the statistical resolution of simulations based on *ab initio* electronic structure methods,[2] hereafter referred to as *ab initio* simulations. The MMBIF method consists of utilizing an auxiliary Markov chain with a known asymptotic distribution based on a molecular mechanics potential to propose trial configurations for an *ab initio*-based Monte Carlo simulation.[2] In this approach, each trial configuration is obtained as the last state in a series of updates based on the molecular mechanics potential starting from the current configuration in the *ab initio* simulation. The proposed configurations are then accepted or rejected in the *ab initio* chain according to the usual Metropolis-Hastings algorithm.[9] If the previous and new trial configurations in the *ab initio* MC chain are denoted by $\mathbf{x}_{old}$ and $\mathbf{x}_{new}$, respectively, the proposed state is accepted with the probability $\min\{1, \exp(-\Delta\Delta E/k_B T)\}$, where $\Delta\Delta E$ is defined to be

$$\begin{aligned}\Delta\Delta E = &(E^{DFT}(\mathbf{x}_{new}) - E^{cl}(\mathbf{x}_{new})) \\ &-(E^{DFT}(\mathbf{x}_{old}) - E^{cl}(\mathbf{x}_{old})),\end{aligned} \tag{1}$$

where $T$ is the temperature, $k_B$ is Boltzmann's constant, and $E^{DFT}(\mathbf{x})$ and $E^{cl}(\mathbf{x})$ are the potential energies of configuration $\mathbf{x}$ calculated by the *ab initio* electronic structure method of choice (here chosen to be density functional theory, abbreviated DFT) and the molecular mechanics (classical) potential, respectively. It is straightforward to show that this acceptance criterion guarantees that the *ab initio* Markov chain has the correct limiting Boltzmann distribution, regardless of the number of molecular mechanics-based updates used to generate the proposed configuration.

The molecular mechanics background simulation produces essentially statistically independent proposal configurations within a fraction of the time necessary for a single DFT energy calculation. As each proposed configuration is independent from the other configurations, the only correlation in the *ab initio* Markov chain comes from the possibility of rejecting the proposed configuration and is a measure of the similarity between the molecular mechanics and *ab initio* potential surfaces. Although construction of a molecular mechanics potential which closely matches the *ab initio* potential is desirable, such a task may prove difficult to realize in practice. It is thus important to study how the accuracy of the molecular mechanics potential energy surface influences the acceptance rate in the *ab initio* chain and hence the statistical efficiency of the simulation. The following conclusions were obtained in a study[2] of the "structural reactions" taking place in a formic acid-water cluster at $T = 200K$ using two reasonable molecular mechanics potentials to guide the *ab initio* simulation.

1. If the agreement between the molecular mechanics and the *ab initio* potentials is only moderate, separating the variables to be updated in the background simulation into several groups will improve the mobility of the *ab initio* MC chain. If possible, one group should contain variables which are strongly correlated. For example, in the case of the proton transfer in a planar molecule like malonaldehyde, the "in-plane" vibrations of the molecule should be relatively uncoupled from the "out-of-plane" motions of the atoms. In general, separating the variables into groups should permit efficient sampling of configurational space when the distribution of states which are poorly estimated by the guiding potential are random, even for molecular mechanics potentials which overestimate or underestimate the energy by a few factors of $k_B T$.

2. Separating the variables to be updated in the generation of trial configurations in the background molecular mechanics simulation usually results in an improved overall acceptance rate of the configurations by the *ab initio* chain. However, when there is an important disagreement between the molecular mechanics and the *ab initio* densities of states which is localized in some region of the state space, long rejection periods could persist. A remedy for this problem is to combine the MMBIF method with another method which generates different Markov chain dynamics. For example, proposed configurations generated from a background simulation based on a different molecular mechanics potential could be used to move the simulation away from the problematic region of the state space. Another means to avoid becoming trapped in phase space would be to use *ab initio* Metropolis updates and the usual Metropolis criteria for acceptance. An equally good solution is to combine importance sampling with sampling based on *ab initio* dynamics when accurate calculation of the forces is possible. In the formic acid-water cluster study, it was demonstrated that separating the variables to be updated in the molecular mechanics potential into groups and using importance sampling techniques in combination with simple Metropolis updates lead to integrated correlation times with a modest molecular mechanics guiding potential which are at most one order of

magnitude larger than in the case where a very good potential is available.

The MMBIF sampling technique has been extended to studies in which nuclear zero-point vibration and tunneling effects are incorporated via centroid transition state theory.[6] Centroid transition state theory[3,4]represents a practical route to calculate approximate quantum rate constants using the path-integral formalism of quantum mechanics[5] and the notion that the reaction rate is governed by the potential of mean force for the centroid reaction coordinate. In the path-integral formalism, quantum particles are mapped onto classical paths $\mathbf{r}(\mathbf{t})$ in imaginary time $t$ with $0 \leq t \leq \hbar/k_B T$, where $\hbar$ is Planck's constant divided by $2\pi$. In practical implementations, discretizations of the closed paths leads to an isomorphism between the path integral formalism and a system of interacting ring polymers with $P$ beads governed by the effective potential

$$U_{eff} = \sum_{i=1}^{N} \frac{P m_i (k_B T)^2}{2\hbar^2} \sum_{j=1}^{P} \left( \mathbf{r}_i^{(j)} - \mathbf{r}_i^{(j+1)} \right)^2 + \frac{1}{P} \sum_{j=1}^{P} U(\mathbf{r}_1^{(j)}, \cdots \mathbf{r}_N^{(j)}), \quad (2)$$

where $N$ is the number of atoms which are treated quantum-mechanically, $P$ is the number of beads in each polymer, $m_i$ is the mass of atom $i$, and $\mathbf{r}_i^{(j)}$ is the position of bead $j$ of atom $i$. In Equation (2), the closure of the Feynman path is imposed by periodic boundary conditions $\mathbf{r}_i^{(j)} = \mathbf{r}_i^{(P+j)}$, and $U(\mathbf{r}_1, \cdots \mathbf{r}_N)$ is the potential energy calculated either by *ab initio* methods or by a molecular mechanics potential. The first term in Equation (2) describes harmonic interactions between the beads and is related to the average quantum kinetic energy. In the limit of an infinite number of beads, the discrete representation of the paths becomes exact and averages over the canonical Boltzmann distribution with effective potential $U_{eff}$ yield the full quantum canonical ensemble averages. In practice, however, only approximately 20 beads are required for each nucleus to obtain converged quantum averages for many systems. The classical limit is recovered as the masses $m_i \to \infty$, in which case the polymer representing the quantum particle collapses onto the center-of-mass or *centroid* of the ring polymer

$$\overline{\mathbf{r}_i} = \frac{1}{P} \sum_{j=1}^{P} \mathbf{r}_i^{(j)}. \quad (3)$$

Although the MMBIF method can be implemented for the path-integral simulation in a straightforward fashion yielding integrated correlation times which are roughly comparable to those obtained in the simulation treating the nuclei classically, importance sampling methods can be used to further reduce the integrated correlation time. In a practical implementation,[6] the efficiency of the *ab initio* path-integral simulation can be increased by generating two coupled, non Markovian simulations in parallel, one with a limiting distribution determined by $U_{eff}^{cl} + U_c^{DFT} - U_c^{cl}$, and the second with the desired limiting Boltzmann path-integral distribution determined by $U_{eff}^{DFT}$. The effective potential energies $U_{eff}^{cl}$ and $U_{eff}^{DFT}$ are calculated via molecular mechanics and *ab initio* potentials, respectively, while $U_c^{cl}$ and $U_c^{DFT}$ represent the classical nuclei molecular mechanics and classical nuclei *ab initio* potentials respectively.

The generalization of the MMBIF method to path-integral simulation is a Monte Carlo method and, in sharp contrast to dynamical methods of sampling the effective distribution, there is no need to use sophisticated staging and thermostating methods to equilibrate the paths. Iftimie and Schofield[6] have demonstrated that if a reasonably good classical description of the *ab initio* potential is available, the MMBIF path-integral simulation method decreases the integrated correlation time of a simple DFT Markov chain path-integral simulation by at least three orders of magnitude and is significantly faster than path-integral molecular dynamics at a given level of statistical uncertainty.

A comparison of present-day molecular dynamics and Monte-Carlo sampling algorithms and their performance was carried out in Ref. 6 where it was demonstrated that the MMBIF sampling approach is at least as efficient as other sampling methods, and, in cases in which a reasonable molecular mechanics guiding potential is available, can lead to reductions in correlation time of several orders a magnitude.

## III. COMPARISON OF CLASSICAL AND *AB INITIO* SECONDARY ISOTOPE EFFECTS

In order to study how the quality of a molecular mechanics description of the reactive energy surface describing the proton transfer in malonaldehyde influences the accuracy of predicted kinetic isotope effects, the two bond evolution theory[10] (BET) molecular mechanics potentials described in detail in Refs. 6 and 11 were utilized. The potentials were constructed as the sum of two terms. The first part of the potential consisted of a quartic, double-well potential in a control parameter $\xi_1$, with $\xi_1$ depending only the coordinates of the atoms directly in-

volved in the bond-breaking and bond-forming processes,

$$\xi_1 = \frac{d_{O_4H_9} - d_{O_7H_9}}{d_{O_4O_7}}. \quad (4)$$

The second term consisted of a sum of harmonic potentials, each depending parametrically on $\xi_1$, to describe the evolution of the bond, bond angle and dihedral motions during the reaction. The two BET molecular mechanics potentials differ in the functional form of the parametric dependence of the carbonylic and enolic bond lengths on $\xi_1$. In the first potential, hereafter called BET1, the minimum energy bond lengths at a fixed value of $\xi_1$ varied linearly with $\xi_1$, while for the second potential, hereafter called BET2, a hyperbolic tangent variation was utilized.

The correct energetics in hydrogen-bonded systems and in systems undergoing proton transfer reactions is difficult to describe even with *ab initio* methods. In particular, DFT studies of weak hydrogen-bonding systems have proved to be particularly difficult and only limited success has been achieved in predicting the geometries and energies for reactant and transition state configurations on the potential energy surface using most exchange-correlation functionals.[12] Care should therefore be exercised when choosing a particular *ab initio* method to calculate reference secondary kinetic isotope effects against which the quality of the classical predictions can be evaluated. The non-local exchange-correlation schemes developed by Proynov, Vela and Salahub[13] have shown particular promise for the description of hydrogen-bonded systems. Sirois et al.[14] have demonstrated that their kinetic-energy dependent exchange functionals (BLAP and PLAP) performed better than all GGA options (BP86, PP86, PW91), BLYP, or other hybrid methods (B3LYP, B3PW91) on systems involving intra-molecular hydrogen bonds. The predictions for equilibrium and transition state geometries as well as the energetics for several test cases agree well with high-quality post-Hartree-Fock coupled cluster CCSD(T) calculations.[14]

The accuracy of the *ab initio* post-Hartree-Fock methods to describe the energetics of intra-molecular hydrogen bonds can be tested by calculating the magnitude of the gas-phase tunneling splitting in malonaldehyde. Although several contradictory results have appeared in the literature over the years,[15] the recent calculations of Benderskii et al[16] using accurate instanton methods[17] estimate the energy difference between reactant and transition state configurations (shown in Figure 1.) to be 4.3 kcal/mol. The results of these calculations are in excellent agreement with DFT calculations using the kinetic-energy dependent PLAP exchange functional, and with the more computationally-intensive CCSD(T) estimates. Moreover, the instanton study of the tunneling splitting[16] predicts an "imaginary" frequency at the transition state of 1290 $cm^{-1}$, in very good agreement with the PLAP prediction of 1270 $cm^{-1}$ obtained in Ref. 11.

For the simulations described in the present work, the energies of different configurations were carried out using a modified version of the LCGTO-DFT program deMon-KS3.4[18,19] using the PLAP exchange-correlation functional. The DFT electronic structure calculations were carried out as in Ref. 14, where the application of DFT electronic structure methods to hydrogen-bonding systems is discussed in detail. A double-$\zeta$ plus polarization (DZVP) orbital basis set was used for all atoms and the convergence level for the SCF (self-consistent field) energy using the auxiliary fitting basis sets[14] was 0.01 kcal/mol.

The centroid potential of mean force for the BET1, BET2 and *ab initio* systems were computed at room temperature ($T = 300K$) using an imaginary-time path-integral representation of all nuclear degrees of freedom and contrasted with similar results obtained when the skeletal carbon atoms in the backbone were treated as classical atoms. The classical treatment of the carbon nuclear degrees of freedom corresponds to studying reaction rates in a malonaldehyde molecule in which the common isotope of the carbon atoms, $^{12}C$, is substituted with very heavy isotopes, denoted $^{h}C$. Centroid transition state theory reaction rates were computed and contrasted using three different choices of reaction coordinate in order to understand the limitations of centroid transition state theory calculations in predicting real kinetic isotope effects. The choices for the reaction coordinate included two reaction coordinates $\xi_1$ and $\xi_2$ depending only on the coordinates of the atoms involved in the bond-breaking and bond-forming processes, where $\xi_1$ was defined in Eq. (4), while $\xi_2$ is defined to be

$$\xi_2 = \left(\mathbf{r}_{H_9} - \frac{\mathbf{r}_{O_4} + \mathbf{r}_{O_7}}{2}\right) \frac{\mathbf{r}_{O_4} - \mathbf{r}_{O_7}}{||\mathbf{r}_{O_4} - \mathbf{r}_{O_7}||}. \quad (5)$$

The third reaction coordinate used in this study is $\xi_3$, which also depends on the position of the carbon atoms

$$\xi_3 = 0.4\xi_1 - \frac{\lambda}{d_0}, \quad (6)$$

where $\lambda = d_{C_3O_4} - d_{C_6O_7}$ and $d_0 = 1$ Å is a scaling length. The form of Eq. (6) is determined by the best linear combination of the variables $\xi_1$ and $\lambda/d_0$

which approximates the projection of the *ab initio* path of steepest descent[20] in the $(\xi_1, \lambda/d_0)$ plane. Centroid TST reaction rates were computed by calculating the potential of mean force for the centroid of the reaction coordinates and the thermal velocities prefactors as described in detail in Ref. 11.

The calculated values of the rate constants for the molecular mechanics and *ab initio* systems for a variety of different isotopic combinations and three choices of reaction coordinate discussed above are shown in Table 1. Several conclusions can be drawn from the analysis of the data in Table 1. First, different choices of reaction coordinates produce overlapping 96% confidence intervals for isotope effects. This fact suggests that kinetic isotope effects obtained with more sophisticated dynamical methods are likely to be in good agreement with the results obtained here using centroid TST and the reaction coordinates mentioned above. Second, calculations of the parameter $r$, where $r$ is defined to be

$$r = \log \frac{k_{^1H,^{12}C}}{k_{^1H,^hC}} / \log \frac{k_{^3H,^{12}C}}{k_{^3H,^hC}} \tag{7}$$

can be carried out based on the rate constant data. The magnitude of $r$ is often used in the physical organic chemistry literature as a measure of the extent to which secondary atoms are involved in tunneling. The value $r = 1$ corresponds to the *rule of geometric mean*, which has been empirically found to be valid[21,22] when reaction rates are calculated using a simple semi-classical transition state theory[23,24] in which tunneling effects are neglected but zero-point energies are incorporated. However, the results of the centroid simulations, which consider tunneling effects in an approximate fashion, predicts different tunneling effects for the BET2 and the BET1 or *ab initio* systems. In particular the results displayed in Table 1 suggest that $r$ is significantly larger than the value predicted by the rule of geometric mean for the BET2 system, yielding a value of $r = 2.6 \pm 0.6$, $r = 2.0 \pm 0.5$, and $r = 2.05 \pm 0.5$ for the $\xi_1$, $\xi_2$, and $\xi_3$ reaction coordinates, respectively. In addition, calculation of semi-classical transition state theory reaction rates using a harmonic description of the potential energy surface in the neighborhood of the minimum energy and transition state configurations show that the breakdown of the rule of geometric mean in the BET2 model cannot be attributed to zero point energy effects. Hence, it appears that for the proton transfer process in the BET2 system, the breakdown of the rule of geometric mean is a signature of important secondary atom tunneling effects. In contrast to the results obtained using the BET2 potential energy surface, no breakdown of the rule of geometric mean is observed for the proton transfer reaction calculations using the BET1 or the *ab initio* DFT potential energy surfaces (i.e. $r = 1.0$ within statistical uncertainties). Indeed, the results in Table 1 indicate that no statistically significant secondary isotope effects are evident in the BET1 and *ab initio* DFT systems.

The molecular mechanics potential energy surfaces BET1 and BET2 differ only in the functional form used for the variation of the bond lengths $C_3O_4$ and $C_6O_7$ with $\xi_1$ along the path of shallowest ascent. This difference translates into slight alterations in the reaction mechanism due to differing degrees of synchronization of the two most important events in the reaction, the transfer of the proton and the response of the backbone to the motion of the proton. The degree of synchronization between the motions of the transferring proton and the carbon backbone atoms can be visualized by examining the path through the configurational space of the system which contributes the most to the (quantum nuclear) free energy of the reactive process, hereafter called the *path of maximum reaction probability*. The projection of the path of maximum reaction probability on the coordinates $\lambda$ and $\xi_1$ for the two molecular mechanics potential energy surfaces BET1 and BET2 have been extracted from the simulation results and are depicted in Figure 2. These coordinates are convenient to analyze since the $\lambda$ coordinate measures the extent of carbon backbone rearrangement while $\xi_1$ gauges the degree of proton displacement. The paths shown in Figure 2 were constructed by finding the most probable value of $\lambda$ for a given value of $\xi_1$ in the simulations after reweighting the data to compensate for the umbrella potental. These data therefore provide a clear indication of the correlation between structural rearrangements of the backbone and the motion of the proton. The results in Figure 2 show that the proton transfer and backbone reorganization events proceed in a concerted fashion at all times for the BET1 system, whereas in the BET2 system the reaction initiates with significant proton motion, while the carbon backbone reorganizes substantially only in the transition state region. The differing degree of carbon backbone motion in the neighborhood of the transition state observed in the simulations of the BET1 and BET2 systems is the likely cause of the difference in the magnitude of secondary atom tunneling effects. In fact, the proton transfer process in the malonaldehyde system can be effectively mapped into a simple two-dimensional model which qualitatively reproduces the heavy atom tunneling behavior as the path of maximum reaction probability changes. The projection of the path of maximum reaction probability in the parameter space spanned by $\lambda$ and $\xi_1$ for the *ab initio* DFT potential reveals

that the marginally significant secondary isotope effects obtained with the *ab initio* potential can be interpreted by means of a reaction mechanism more similar to the BET1 than to the BET2 system.

## IV. CONCLUSIONS

Two important theoretical questions pertaining to accurate studies of proton transfer reactions have been investigated in this study. First, it has been demonstrated that the use of molecular mechanics potentials to study secondary kinetic isotope effects can result in artifacts unless special care is exercised in designing the molecular mechanics potential. In particular, it has been demonstrated that an unphysical molecular mechanics potential with an incorrect projection of the path of steepest descent on degrees of freedom involving secondary atom motion can result in erroneous secondary atom tunneling effects predictions. One easy means to address this problem would be to ensure that molecular mechanics potentials designed by fitting parameters from accurate electronic structure potentials correctly describe not only the energetics and structure of the minimum energy and transition state configurations, but also their eigenfrequencies and eigenmodes. In particular the projection of the eigenmode corresponding to the "imaginary frequency" at the transition state configuration on different primary and secondary atom motions should be carefully investigated.

The second theoretical question addressed here concerns the partitioning of the nuclear degrees of freedom of a reactive system into quantum and classical components. Although it is generally believed that primary atoms directly involved in the bond-breaking and bond-forming processes should be treated quantum-mechanically, one might expect that treating heavy secondary atoms in a classical fashion would introduce only negligible systematic errors in the calculation of reaction rates. However this is clearly not the case when collective motions of secondary atoms play a critical role in the reaction mechanism. The BET2 system, where quantization of the nuclear degrees of freedom of the carbon atoms increased the tautomerization rate by a factor of 5, is an example of such a scenario. For systems exhibiting important heavy atom tunneling, the neglect of the quantum dispersion of the heavy nuclei can lead to errors in the calculation of rate constants of up to a factor of 10 and may well be the most significant source of systematic error in the calculation of the rate constant. Although significant secondary atom nuclear quantum effects were not observed in the model proton transfer reaction studied here when the *ab initio* DFT potential was used, secondary atom tunneling is likely to be important in real processes in which the reaction mechanism involves considerable motion of secondary atoms in the transition state region. It is therefore important to treat the quantum nuclear effects of all secondary atoms which move cooperatively as a chemical process proceeds.

The centroid TST calculations using *ab initio* electronic structure calculations reported in this study have been performed using the molecular mechanics based importance function method. This *ab initio* Monte Carlo method is easier to implement and is computationally more efficient than other sampling schemes, such as *ab initio* Car-Parinello molecular dynamics[25] or its path-integral extensions,[26] provided a reasonable molecular mechanics description of the system in study exists. Recent progress in the design of molecular mechanics potentials to describe chemical reactions,[27] and, in particular, proton transfer processes, should be quite useful in providing reasonable molecular mechanics guiding potentials which can be successfully used to improve the statistical resolution of *ab initio* simulations.


[1] See for example E. Buncel and W. H. Saunders, Jr., *Isotopes in organic chemistry*, Vol. 8, *Heavy atom Isotope Effects*, Elsevier, 1992, and Vol. 7, *Secondary and Solvent Isotope Effects*, Elsevier, 1987.

[2] R. Iftimie, D. Salahub, D. Wei and J. Schofield, J. Chem. Phys. **113**, 4852, (2000).

[3] M. J. Gillan, J. Phys. C **20**, 3621, (1987).

[4] G. A. Voth, D. Chandler and W. Miller, J. Chem. Phys. **91**, 7749 (1989); G. A. Voth, J. Phys. Chem. **97**, 8365 (1993).

[5] R. P. Feynman and A. R. Hibbs, *Quantum Mechanics and Path Integrals*, (McGraw-Hill, New York, 1965).

[6] R. Iftimie and J. Schofield, J. Chem. Phys., **114**, (2001).

[7] M. E. Tuckerman and A. Hughes in *Classical and Quantum Dynamics in Condensed Phase Simulations*, B. J. Berne, G. Ciccotti and D. F. Coker, eds., World Scientific, Singapore, 1998; M. E. Tuckerman, B. J. Berne, G. J. Martyna and M. L. Klein, J. Chem. Phys. **99**, 2796, (1993).

[8] D. Gerritzen and H.-H. Limbach, J. Am. Chem. Soc. **106**, 869 (1984).

[9] J. S. Liu, *Monte Carlo Strategies in Scientific Computing*, (Springer-Verlag, New York, 2001).

[10] X. Krokidis, V. Goncalves, A. Savin and B. Silvi, J. Phys. Chem. A **102**, 5065 (1998); B. Silvi and A. Savin, Nature (London) **371**, 683 (1994).

[11] R. Iftimie and J. Schofield, J. Chem. Phys. (in press).

[12] V. Barone and C. Adamo, J. Chem. Phys. **105**, 11007, (1996).
[13] E. I. Proynov, A. Vela and D. R. Salahub, Chem. Phys. Lett. **230**, 419, (1994); **234**, 462(E), (1995).
[14] S. Sirois, E. I. Proynov, D. T. Nguyen and D. R. Salahub, J. Chem. Phys. **107**, 6770, (1997).
[15] Z. Smedarchina, W. Siebrand and M. Z. Zgierski, J. Chem. Phys. **103**, 5326 (1995).
[16] V. A. Benderskii, E. V. Vetoshkin, J. S. Irgibaeva and H. P. Trommsdorff, Chem. Phys. **262**, 393 (2000).
[17] V. A. Benderskii, E. V. Vetoshkin, L. von Laue and H. P. Trommsdorff, Chem. Phys. **219**, 119 (1997).
[18] E. I. Proynov, S. Sirois and D. R. Salahub, Int. J. Quantum Chem. **64**, 427, (1997).
[19] For details on the deMon quantum chemistry package, see http://www.cerca.umontreal.ca/deMon/Welcom_f.html.
[20] K. Fukui, J. Phys. Chem. **74**, 4161 (1970); K. Fukui and H. Fujimoto, *Frontier Orbitals and Reaction Paths, Selected Papers of Kenichi Fukui*, (World Scientific, Singapore, 1997).
[21] J. Biegeleisen, J. Chem. Phys. **23**, 2264 (1995).
[22] J. Ricker and J. Klinman, JACS, **121**, 1997 (2001); A. Kohen, R. Cannio, S. Bartolucci and J. P. Klinman, Nature, **399**, 496 (1999); B. J. Bahnson, T. D. Colby, J. K. Chin, B. M. Goldstein and J. P. Klinman, Proc. Natl. Acad. Sci. USA, **94**, 12797 (1997); Y. Cha, C. J. Murray and J. P. Klinman, Science, **243**, 1325 (1989).
[23] W. H. Saunders, Jr., J. Am. Chem. Soc. **107**, 164 (1985), and references therein.
[24] R. P. Bell, *The proton in chemistry*, Chapman and Hall, London, Second Edition, 1973.
[25] R. Car and M. Parrinello, J. Chem. Phys. **80**, 860 (1985); R. Car and M. Parrinello, Phys. Rev. Lett. **55**, 2471 (1985).
[26] M. E. Tuckerman, D. Marx, M. L. Klein and M. Parrinello, J. Chem. Phys. **104**, 5579 (1996).
[27] T. Albu, J. C. Corchado and D. G. Truhlar, J. Phys. Chem. A (in press).

## Figure Captions

Figure 1. The proton transfer tautomerization reaction in the enol form of malonaldehyde. The product state (not shown) is chemically equivalent to the reactant state.

Figure 2. A plot of the maximum density of points in the $(\xi_1, \lambda)$ plane for the BET1 (solid line) and BET2 (dashed line) simulations. The maximum density of points for the *ab initio* simulation (not shown) follows the same profile as that of the BET1 simulation. $\xi_1$ is the reaction coordinate defined in Equation (4), and $\lambda = d_{C_3O_4} - d_{C_6O_7}$ is the difference between the carbonyl and enolic bond lengths. $\xi_{\rm prod}$ and $\lambda_{\rm prod}$ represent the $\xi_1$ and $\lambda$ values calculated for the product configurations.

TABLE I. 96% confidence intervals for centroid transition state rate constants using the *ab initio*, BET1 and BET2 potentials. Note that the secondary isotope effects are statistically negligible for the *ab initio* and BET1 molecular mechanics potential for all three choices of reaction coordinates and irrespective of the mass of the transferring proton. The secondary kinetic isotope effects for the BET2 potential are statistically resolvable only for $^1H$.

| Potential surface | Reaction coordinate | Isotopic Substitution | $^1H$ | $^3H$ |
|---|---|---|---|---|
| *ab initio* | $\xi_1$ | $^{12}C$ | $3.82 \cdots 5.15 \times 10^{11}$ | |
| | | $^hC$ | $3.00 \cdots 3.89 \times 10^{11}$ | |
| | $\xi_2$ | $^{12}C$ | $3.41 \cdots 4.83 \times 10^{11}$ | |
| | | $^hC$ | $2.43 \cdots 3.11 \times 10^{11}$ | |
| | $\xi_3$ | $^{12}C$ | $4.42 \cdots 5.94 \times 10^{11}$ | |
| | | $^hC$ | $3.46 \cdots 4.55 \times 10^{11}$ | |
| BET 1 | $\xi_1$ | $^{12}C$ | $6.14 \cdots 7.42 \times 10^{11}$ | $2.28 \cdots 2.67 \times 10^{11}$ |
| | | $^hC$ | $5.11 \cdots 6.08 \times 10^{11}$ | $2.01 \cdots 2.43 \times 10^{11}$ |
| | $\xi_2$ | $^{12}C$ | $7.03 \cdots 8.10 \times 10^{11}$ | $2.43 \cdots 2.81 \times 10^{11}$ |
| | | $^hC$ | $5.63 \cdots 6.91 \times 10^{11}$ | $2.21 \cdots 2.65 \times 10^{11}$ |
| | $\xi_3$ | $^{12}C$ | $6.26 \cdots 7.65 \times 10^{11}$ | $2.53 \cdots 2.81 \times 10^{11}$ |
| | | $^hC$ | $5.84 \cdots 7.28 \times 10^{11}$ | $2.11 \cdots 2.48 \times 10^{11}$ |
| BET 2 | $\xi_1$ | $^{12}C$ | $2.53 \cdots 3.11 \times 10^{11}$ | $0.94 \cdots 1.16 \times 10^{11}$ |
| | | $^hC$ | $1.18 \cdots 1.46 \times 10^{11}$ | $0.98 \cdots 1.21 \times 10^{11}$ |
| | $\xi_2$ | $^{12}C$ | $3.43 \cdots 4.25 \times 10^{11}$ | $1.28 \cdots 1.59 \times 10^{11}$ |
| | | $^hC$ | $0.88 \cdots 1.29 \times 10^{11}$ | $0.85 \cdots 1.38 \times 10^{11}$ |
| | $\xi_3$ | $^{12}C$ | $2.67 \cdots 3.27 \times 10^{11}$ | $1.08 \cdots 1.32 \times 10^{11}$ |
| | | $^hC$ | $1.32 \cdots 1.64 \times 10^{11}$ | $1.06 \cdots 1.32 \times 10^{11}$ |

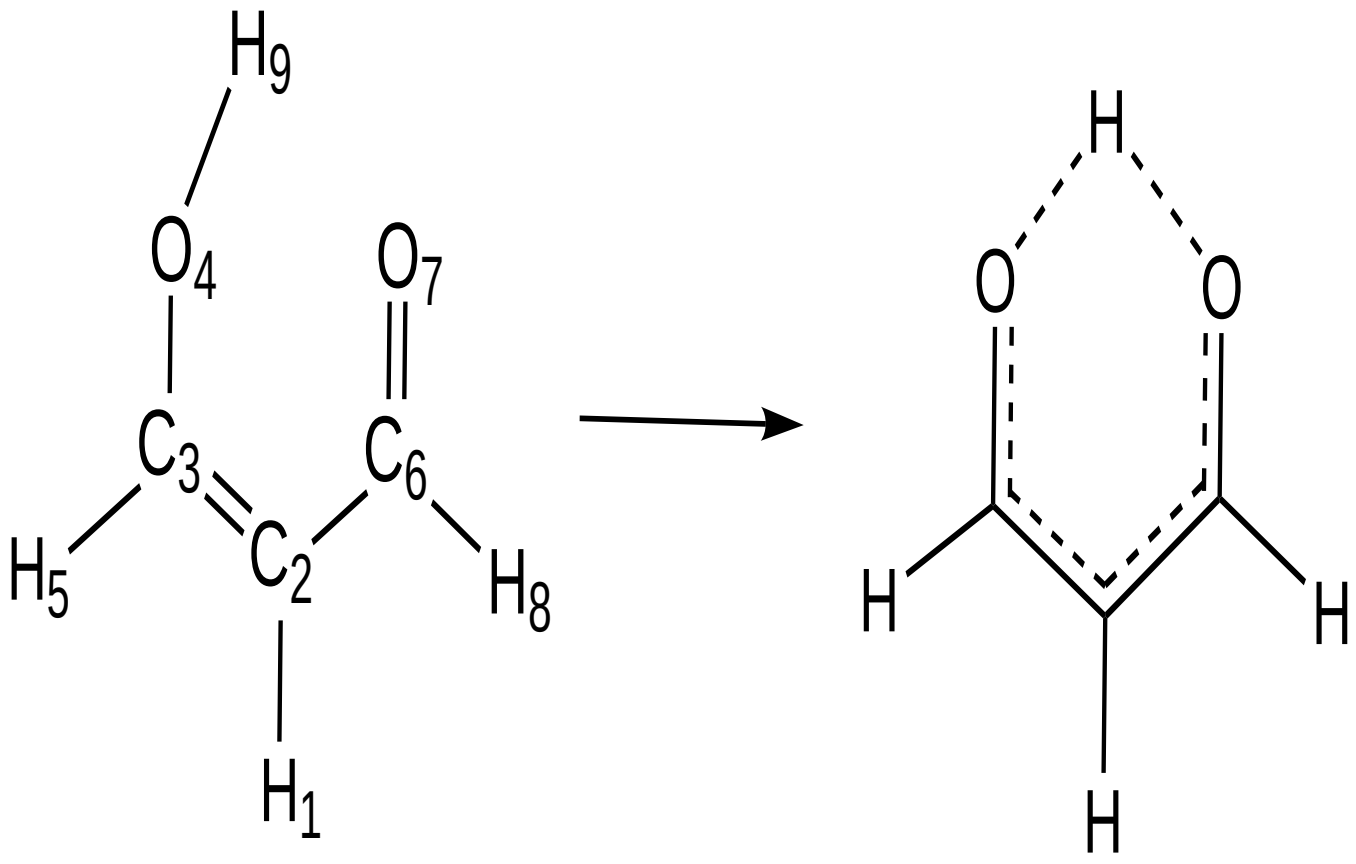


Reactant

Transition State

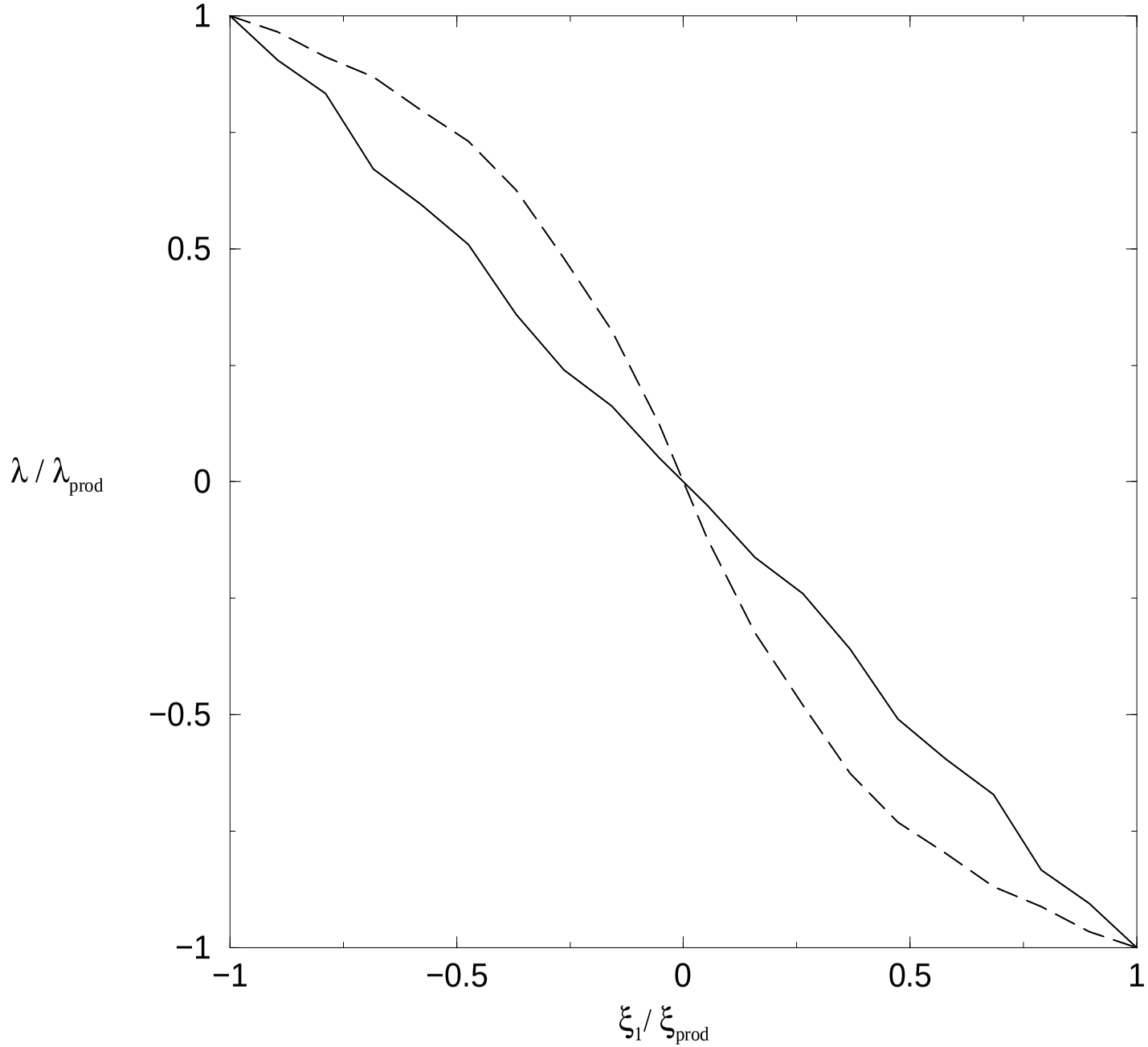


Figure 2.